THE FREE ELECTRON LASER ACTIVITIES AT THE BUDKER INP

N. A. VINOKUROV

Budker Institute of Nuclear Physics,
11 Ac. Lavrentyev Prosp, 630090, Novosibirsk, Russia

The free electron laser activity in the Budker Institute of nuclear physics is briefly described.

1 Introduction

Like all other lasers, free electron lasers (FELs) are generators or amplifiers of the coherent electromagnetic radiation of the optical range. Their working media is the ultrarelativistic (i.e., moving with speed, close to the speed of light) electron beam, passing through a periodic alternating transverse magnetic field. A special magnet creating such a field is called an undulator and radiation of an electron flying in such field is called the undulator radiation. As in other lasers, an electromagnetic wave can be amplified in the radiating media due to the stimulated emission of radiation phenomenon. Therefore one can say, that the principle of operation for the FEL is based on the stimulated undulator radiation. The particular mechanism of the stimulated undulator radiation is the longitudinal bunching of electrons, i.e. appearing in the electron beam compactions with a space period approximately equal to the radiation wavelength (more detailed information on FELs is in books[1,2]).

FELs have some features that distinguish them among other lasers. Firstly, the radiation wavelength is determined by the undulator parameters and electron energy, hence it can be of practically any value - from millimeters to nanometers - and can be continuously tuned. Secondly, the existence of the electron beams with the average power in the order of tens of megawatts allows to create FELs of average power up to several megawatts. Thirdly, relatively small optical density and «simplicity» of the working media allow one to obtain radiation with extremely small (diffraction limited) angular divergence. This distinguished properties determine possible applications of FELs: spectroscopy, laser photochemistry, isotope separation, laser medicine, power beaming to satellites, and so on.

The first FEL[3], built by the group of J. M. J. Madey in 1976, inspired the great interest to these devices around the whole world. The Budker Institute of nuclear

physics is involved to the FEL activity since 1977, when the papers by V. N. Baier and A. I. Milstein on the explanation of the FEL principle of operation in the terms of classical mechanics[4] and by A. N. Skrinsky and N. A. Vinokurov on the optical klystron[5] appeared.

2 The optical klystron

The last paper was the result of the understanding of the electron dynamics in FEL and invented the modification of the conventional undulator. From the point of view of the electron motion this new device is similar to the well-known RF tube - the klystron. We will discuss it in more details now to clarify the FEL operation.

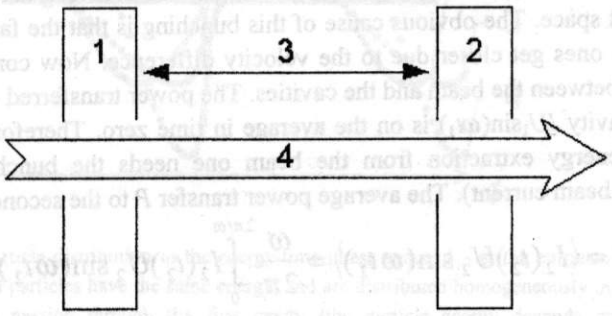

Fig. 1: The RF klystron. 1, 2 - the cavities, 3 - the drift space, 4 - the electron beam.

The simplest radiofrequency (RF) klystron consists of two cavities with the drift space between them (Fig. 1). The unbunched monoenergetic electron beam passes through the first cavity. If the fundamental eigenmode E_{010} is excited in the cavity at frequency ω (by some external RF generator, for example), the particles, entering the drift space will have different energies E, dependently on the moment of time t_1, when they pass through the cavity:

$$E - E_0 = eU_1 \sin(\omega t_1), \qquad (1)$$

where E_0 is the initial particle energy, e is the electron charge, and U_1 is the amplitude of the accelerating voltage. As the particle velocity v depends on energy, the time of flight through the drift space of the length L -

$$T = \frac{L}{v(E)} \approx T_0 - \left(\frac{dT}{dE}\right)_0 eU_1 \sin(\omega t_1) \qquad (2)$$

depends on t_1. Here $T_0=L/v(E_0)$ and the coefficient $(dT/dE)_0$ is referred to as the longitudinal dispersion and characterizes the energy dependence of the flight

time. For the empty drift space $(dT/dE)_0=-Lm^{-1}c^{-3}(\gamma_0^2-1)^{-3/2}$, where m is the electron mass, and $\gamma_0=E_0/mc^2$. Correspondingly, the arrival time to the second cavity is $t_2=t_1+T_0-(dT/dE)_0\, eU_1\sin(\omega t_1)$. Consider two particles, which passed through the first cavity at slightly different times t_1 and t_1+dt_1. The time interval between their arrival to the second cavity is $dt_2=dt_1[1-\omega(dT/dE)_0 eU_1\cos(\omega t_1)]$. According to the conservation of the number of particles (the electric charge), enclosed inside the interval dt_1, $I_1(t_1)dt_1=I_2(t_2)dt_2$, where I_1 and I_2 are the currents in the first and second cavities correspondingly. For the initially unbunched beam $I_1=I$ is constant, but

$$I_2 = I\left(\frac{dt_2}{dt_1}\right)^{-1} = I\left[1-\omega\left(\frac{dT}{dE}\right)_0 eU_1\cos(\omega t_1)\right]^{-1} \qquad (3)$$

depends on time periodically with the period $2\pi/\omega$. Thus, one can say, that due to the particle energy modulation in the first cavity the bunching take place at the end of the drift space. The obvious cause of this bunching is that the faster particles and the slower ones get closer due to the velocity difference. Now consider the energy exchange between the beam and the cavities. The power transferred from the beam to the first cavity $IU_1\sin(\omega t_1)$ is on the average in time zero. Therefore to provide the effective energy extraction from the beam one needs the bunched beam (time-dependent beam current). The average power transfer P to the second cavity is

$$\Delta P = \langle I_2(t_2)U_2\sin(\omega t_2)\rangle = \frac{\omega}{2\pi}\int_0^{2\pi/\omega} I_2(t_2)U_2\sin(\omega t_2)dt_2 =$$
$$\frac{\omega}{2\pi}IU_2\int_0^{2\pi/\omega}\sin(\omega t_2)dt_1 = IU_2 J_1\left[\omega\left(\frac{dT}{dE}\right)_0 eU_1\right]\sin(\omega T_0) \qquad (4)$$

where J_1 is the Bessel function. It is maximal for the optimal length of the drift space, when $\sin(\omega T_0)=-1$. The meaning of this condition is deceleration of the bunches centered at $\omega t_1=(2n+1)\pi$. The particle distribution in the phase space E,t at different points of the klystron is shown in Fig.2.

To use the similar way of particle deceleration (in average) for short wavelengths one have to change all components of the device.

Firstly, it needs to replace the accelerating gap, which changes the particle energy. The possible substitution is the undulator, invented first by V. L. Ginzburg[6], and the electromagnetic wave. Planar undulator is the magnet, which creates in the horizontal (x,z) plane the vertical magnetic field $B_y = B_0\cos(k_w z)$ with the period $2\pi/k_w$. For certain initial conditions the trajectory of the ultrarelativistic ($\gamma>>1$) electron in this field may be written in form:

$$x \approx -\frac{K}{\gamma k_w}\cos(k_w z), \tag{5}$$

where $K = eB_0 k_w / mc^2$ is so-called deflection parameter. Let the electromagnetic wave with the horizontal electric field $E_z = A\cos(kz - \omega t)$ propagates along z axis, $k = \omega/c$ (Fig. 3).

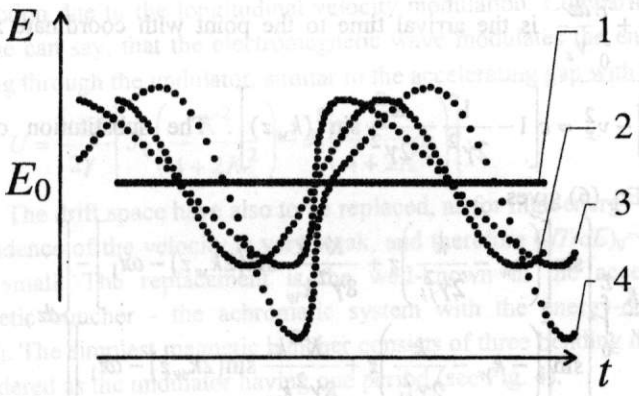

Fig. 2: The particle distribution in the energy-time phase space. 1 - at the entrance to the first cavity (all particles have the same energy, and are distributed homogeneously in time), 2 - after the passing through the first cavity (the particle energy depends on time sinusoidally, but the time distribution is still homogeneous), 3 - at the end of the drift space (the arrival times are shifted depending on the energy deviation, therefore the bunching occure), 4 - after the passing through the second cavity (the electron bunches are decelerated, and therefore the average particle energy is decreased).

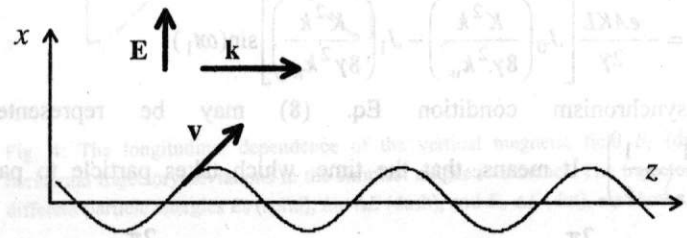

Fig. 3: The particle trajectory in the planar undulator.

Considering this wave field as the small perturbation, one can find that in the first order approximation the variation of the particle energy

$$E - E_0 = \int e\mathbf{E}d\mathbf{s} = \frac{eAK}{\gamma}\int_0^L \cos(kz - \omega t)\sin(k_w z)dz\,, \qquad (6)$$

where $t = t_1 + \int_0^z \frac{dz}{v_z}$ is the arrival time to the point with coordinate z, and $v_z = \sqrt{c^2\left(1-\frac{1}{\gamma^2}\right) - v_x^2} \approx c\left[1 - \frac{1}{2\gamma^2} - \frac{K^2}{2\gamma^2}\sin^2(k_w z)\right]$. The substitution of the expression for t to Eq. (6) gives

$$E - E_0 = \frac{eAK}{2\gamma}\int_0^L \left\{\begin{array}{l}\sin\left[\left(k_w - \frac{k}{2\gamma_{//}^2}\right)z + \frac{K^2 k}{8\gamma^2 k_w}\sin(2k_w z) - \omega t_1\right] - \\ \sin\left[\left(-k_w - \frac{k}{2\gamma_{//}^2}\right)z + \frac{K^2 k}{8\gamma^2 k_w}\sin(2k_w z) - \omega t_1\right]\end{array}\right\}dz\,, \qquad (7)$$

where $\gamma_{//} = \gamma\left(1 + K^2/2\right)^{-1/2}$ is the relativistic factor, corresponding to the z-component of the electron velocity, averaged over the undulator period. For the long undulator ($k_w L >> 1$) both terms under the integral Eq. (7) oscillates, except of the case, when

$$k = 2\gamma_{//}^2 k_w \qquad (8)$$

and the first term gives the main contribution:

$$E - E_0 = -\frac{eAKL}{2\gamma}\left[J_0\left(\frac{K^2 k}{8\gamma^2 k_w}\right) - J_1\left(\frac{K^2 k}{8\gamma^2 k_w}\right)\right]\sin(\omega t_1)\,. \qquad (9)$$

The synchronism condition Eq. (8) may be represented as $\frac{2\pi}{\omega} = \frac{2\pi}{k_w}\left(\frac{1}{\langle v_z\rangle} - \frac{1}{c}\right)$. It means, that the time, which takes particle to pass one undulator period $\frac{2\pi}{k_w\langle v_z\rangle}$, is exactly one wave period $\frac{2\pi}{\omega}$ more, than the corresponding time for light $\frac{2\pi}{k_w c}$. Choosing the proper particle energy according to

Eq. (8), one can arrange effective interaction of particle and wave of any, even very high, frequency. The meaning of the first factor in Eq. (9) is obvious: the average projection of the Lorentz force $e\mathbf{E}$ to the particle trajectory tangent vector, tilted by the K/γ angle from the z axis, is multiplied to the undulator length L. The argument of the Bessel functions in Eq. (9) may be simplified using Eq. (8): $K^2/(4+2K^2)$. For any K it varies from zero to 0.5, and, correspondingly, the value of the square bracket in Eq. (9) varies from one to 0.7. This factor shows the reduction of the wave-particle interaction due to the longitudinal velocity modulation. Comparing Eq. (1) and Eq. (9) one can say, that the electromagnetic wave modulates the energies of particles, passing through the undulator, similar to the accelerating gap with the voltage

$$U = \frac{AKL}{2\gamma}\left[J_0\left(\frac{K^2}{4+2K^2}\right) - J_1\left(\frac{K^2}{4+2K^2}\right)\right]. \qquad (10)$$

The drift space have also to be replaced, as for high energy electron the energy dependence of the velocity is very weak, and therefore $(dT/dE)_0 = -Lm^{-1}c^{-3}(\gamma_0^2-1)^{-3/2}$ is very small. The replacement is the well-known in the accelerator technology magnetic buncher - the achromatic system with the energy-dependent trajectory length. The simplest magnetic buncher consists of three bending magnets and may be considered as the undulator having one period (see Fig. 4).

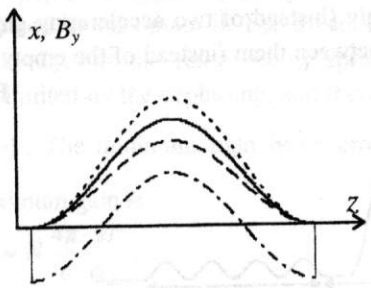

Fig. 4: The longitudinal dependence of the vertical magnetic field B_y (dash-dot) and horizontal trajectory deviations in the simplest magnetic buncher. The trajectories for three different particle energies E_0 (solid), $E_0+\Delta E$ (dash), and $E_0-\Delta E$ (dot), are shown.

Assuming the deflection angle dx/dz to be small one can write the simple equation for the trajectory:

$$\frac{d^2x}{dz^2} = -\frac{eB_y(z)}{\gamma mvc}. \tag{11}$$

Then for the whole buncher it is easy to obtain the conditions of zero bend angle $\int_{-\infty}^{\infty} B_y dz = 0$ and zero coordinate shift $\int_{-\infty}^{\infty}\int_{-\infty}^{z} B_y(z)dz\,dz = 0$, and the path difference due to curvature of the trajectory

$$\Delta S = \frac{1}{2}\int_{-\infty}^{\infty}\left(\frac{dx}{dz}\right)^2 dz = \frac{1}{2}\left(\frac{e}{\gamma mvc}\right)^2 \int_{-\infty}^{\infty}\left[\int_{-\infty}^{z} B_y(z)dz\right]^2 dz. \tag{12}$$

The longitudinal dispersion of the buncher having length L_b is

$$\frac{dT}{dE} = \frac{1}{v}\frac{d(L_b + \Delta S)}{d\mathrm{E}} - \frac{L_b}{v^2}\frac{dv}{dE} \approx -\frac{2}{Ec}\left(\Delta S + \frac{L_b}{2\gamma^2}\right). \tag{13}$$

According to Eq. (13) one can say, that the magnetic field add to the «effective length of the drift section» the value $2\gamma^2\Delta S = \left(\frac{e}{mc^2}\right)^2 \int_{-\infty}^{\infty}\left[\int_{-\infty}^{z} B_y(z)dz\right]^2 dz$, which increase the longitudinal dispersion dramatically.

Thus, the magnetic system of the optical klystron consists of two undulators with lengths L_1 and L_2 correspondingly (instead of two accelerating gaps in the RF klystron), and the magnetic buncher between them (instead of the empty drift space). The el

Fig. 5.

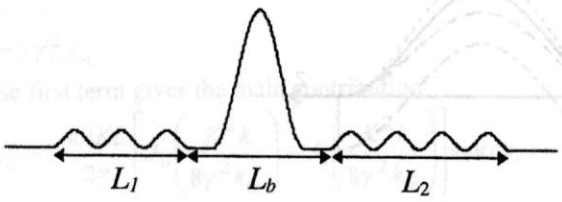

Fig. 5: The electron trajectory in the optical klystron.

To calculate the power transfer from the electron beam to the electromagnetic wave one can use Eq. (4) and Eq. (10). As the same electromagnetic wave is used to change the particle energy in both undulators, the optimal phasing take place for $\omega\frac{L_b + \Delta S}{v} - kL_b \approx k\left(\frac{L_b}{2\gamma^2} + \Delta S\right) = \left(2n - \frac{1}{2}\right)\pi$ and may be arranged by the proper

choice of the value of magnetic field in the buncher (it is easy, as typically $k\Delta S>>1$). For the small wave amplitude the Bessel function in Eq. (4) may be expanded as $J_1(x)\approx x/2$, then

$$\Delta P = -\frac{eI}{2}\omega\left(\frac{dT}{dE}\right)_0\left\{\frac{AK}{2\gamma}\left[J_0\left(\frac{K^2}{4+2K^2}\right)-J_1\left(\frac{K^2}{4+2K^2}\right)\right]\right\}^2 L_1L_2. \qquad (14)$$

Taking into account the longitudinal dispersion of undulators, one have to add $-\frac{L_1+L_2}{2\gamma_{//}^2 Ec}$ to the value of $\left(\frac{dT}{dE}\right)_0$ from Eq. (13).

For the collimated light beam (the Gaussian beam, for example) with power P_0 and cross-section $S=\frac{8\pi P_0}{A^2c}$ the gain (for thin electron beam) is defined as the relative increase of the power in the light beam:

$$G=\frac{\Delta P}{P_0}=-4\pi\frac{eI}{cS}\omega\left(\frac{dT}{dE}\right)_0\left\{\frac{K}{2\gamma}\left[J_0\left(\frac{K^2}{4+2K^2}\right)-J_1\left(\frac{K^2}{4+2K^2}\right)\right]\right\}^2 L_1L_2 \qquad (15)$$

If the light is propagating back and forth between two mirrors with R_1 and R_2 reflectivities, the light power will grows in time exponentially, when the gain is big enough: $(1+G)R_1R_2>1$. Typically the gain is significantly less than one, and the efforts are aimed to maximize it. For given full length of the device the gain is maximal at $L_1=L_2$. For the finite energy spread σ_E the value of the longitudinal dispersion is limited by the dephasing, and therefore the maximum gain take place at $\omega\frac{dT}{dE}\sigma_E=-1$. The minimum light beam cross-section S is approximately $\pi L_1/k$. Thus the maximum gain is

$$G_{\max}\approx N\frac{4\pi}{c}\frac{eI}{\sigma_E}, \qquad (16)$$

where $N=k_wL_1/2\pi$ is the number of periods in each undulator. The optical klystron is useful for the storage ring FEL, where the energy spread is low and the number of undulator periods is limited. Therefore all storage ring FELs use the optical klystron scheme.

3 The high power FEL

The understanding of FEL physics led to the invention and experimental investigation of the optical klystron[5,9], the hybrid permanent magnet undulator[10] and other new devices and techniques[11,12]. Correspondingly, the use of these inventions in

the experiments on the VEPP-3 storage ring enables us to achieve the extremely short (0.24 micron) wavelength[13], extremely narrow ($3 \cdot 10^{-6}$) bandwidth[14] and other interesting results[15,16]. Nevertheless, the storage ring FELs suffer from the intrinsic power limitation. This is the well-known Renieri limit[7,8,17,18], caused by the increase of the beam energy spread during the interaction with light in the undulator. Therefore for the kilowatt average power range FEL one can not use a storage ring[19].

3.1 Energy recovery

Typically, the efficiency of the conversion of the beam power to the radiation power is rather small in an FEL, being typically not more than a few percent. For high power applications, therefore, it is necessary to recover the beam power after the FEL interaction. The main reason for the energy recovery, except of simple energy saving, is the dramatic reduction of the radiation hazard at the beam dump.

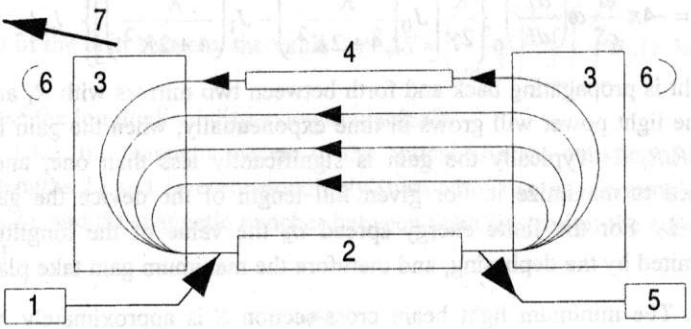

Fig. 6: The scheme of the FEL with the accelerator-recuperator. 1-injector; 2-RF accelerating structure; 3-180-degree bends; 4-FEL magnetic system; 5-beam dump; 6-mirrors; 7 output light beam.

One of the possible methods of the beam energy recovery is to return the beam to the RF accelerating structure, which was used to accelerate it[8,20]. If the length of path from the accelerator through the FEL to the accelerator is chosen properly, the deceleration of particles will occur instead of acceleration, and therefore the energy will return to the accelerating RF field (in other words, the beam will excite RF oscillations in the accelerating structure together with the RF generator). Such a mode of accelerator operation was demonstrated at the Stanford HEPL[21]. An obvious development of such an approach is the use of multipass recirculator[22,23] instead of simple linac. By increasing of the number of passes, cost and power consumption can

be reduced. However, the threshold currents for instabilities also decrease, so the "optimal" number of passes exists[24]. The general scheme of such FEL is shown in Fig. 6.

The electron beam from the injector 1 enters the RF accelerating structure 2. After the first acceleration in the accelerating structure the beam passes through the magnetic system (bends 3 and focusing quadrupoles), which returns it to the accelerating structure for the second time. To have the acceleration of the beam at each pass though the accelerating structure it is enough to choose the orbit lengths to be integer of the RF wavelength (approximately). After several passes through the accelerating structure the beam reach the required energy and enters the FEL magnetic system 4, which is installed in the straight section of the last orbit. Here the small (about 1%) amount of the electron beam power is converted to the light. The exhaust beam returns to the accelerating structure. To provide a deceleration of the exhaust beam instead of an acceleration, the length of the last orbit is approximately half-integer of the RF wavelength. Due to the relatively small energy difference the decelerating beam follows almost the same orbits, as the accelerated one. Finally, the low-energy exhaust beam is absorbed in the beam dump 5. Some desirable features of an accelerator-recuperator are listed below.

1. The ejection (and, correspondingly, the injection) energy is to be less than 10 MeV, to avoid neutron generation in the beam dump.

2. The electron optical system has to provide proper focusing for the accelerating and the decelerating beams. It is not so trivial, as each orbit, except for the last one, is used to transport two beams (accelerating and decelerating) with the different initial conditions simultaneously, and there are many beams with very different energies inside the linac.

3. Energy acceptance is to be a few percents or larger to decelerate the spent electron beam. This can be achieved by employing magnetic system consisting of achromatic bends with low enough transverse dispersion function inside.

4. It is preferable to have a zero transverse dispersion function in the straight line sections to allow the optimization of the betatron phase advances at each orbit to increase the threshold current for the transverse beam breakup.

5. The frequency of the RF system tends to be low to decrease the longitudinal and transverse impedances and increase the longitudinal acceptance. Another advantage of low frequencies is the possibility of using the separated (uncoupled) RF resonators with individual tunes of fundamental and asymmetric modes.

To preserve low transverse emittance it is preferable to have a high peak current only at high energies. So the rotation in the longitudinal phase space by $\pi/2$, $3\pi/2$,... may be useful.

The high power infrared FEL for the Siberian center of photochemical research, which is under construction now, is the implementation of this approach.

3.2 Accelerator-recuperator

The accelerator - recuperator layout is shown in Fig. 7. The 2 MeV electron beam from the injector passes 8 times through the accelerating structure, getting the 98 MeV energy, and comes to the FEL, installed in the last straight section. After the loss of about 1% of its power the beam passes 8 times more through the accelerating structure, returning the power, and comes to the beam dump at the injection energy.

Some parameters of the accelerator are listed in the table:

RF wavelength, m	1.66
Number of RF cavities	16
Amplitude of accelerating voltage at one cavity, MV	0,8
Number of orbits	8
Injection energy, MeV	2
Final electron energy, MeV	98
Bunch repetition frequency, MHz	2 - 22,5
Average current, mA	4 - 50
Final electron energy dispersion, %	0,2
Final electron bunch length, ps	20 - 100
Final peak electron current, A	100 - 20

The 300 keV electron gun of the injector produces the 1 ns electron bunches with a repetition frequency up to 22.5 MHz. It has the DC power supply (rectifier) and termionic cathode with the greed. After passing the modulating RF cavity, the electron bunch is compressed in a drift section down to 200 ps and accelerated up to 2 MeV in the next two RF cavities. After that electrons are injected into the common straight section of the microtron - recuperator, using two pairs of the identical bending magnets with opposite magnetic field signs. At the entrance to the main accelerating system the bunch length is 100 ps. The project of the 300 keV photoinjector was developed[25] to replace the thermionic gun in future.

The accelerating structure consists of 16 RF cavities. Each cavity has mechanical tunings for the fundamental and high order modes. The effective accelerating voltage is 0.8 MV at the thermal power consumption about 0.1 MW. So, the total RF power is near 2 MW. The details of the RF system design and tests were described in paper[26].

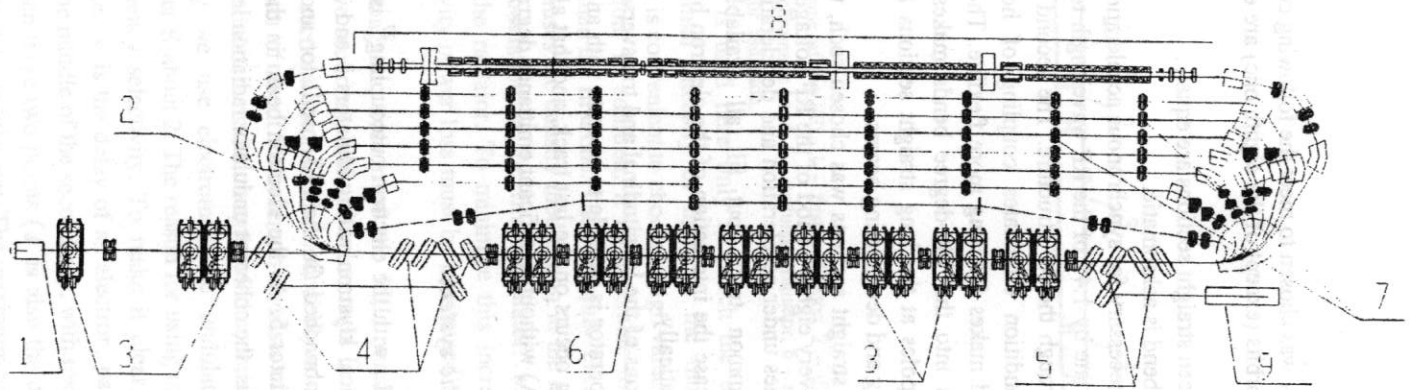

Fig. 7: Scheme of the microtron-recuperator (1 - electron gun; 2 - bending magnets; 3 - RF resonators; 4,5 - injection and extraction magnets; 6 - focusing solenoids; 7 - straight sections with the quadrupole lenses; 8 - FEL magnetic system; 9 - beam dump).

The orbit geometry was chosen to meet the following conditions:

the lengths of all orbits (except of the eighth one) are equal to integer number of the RF wavelength;

the distances between straight sections are equal;

each 180 - degree bend is achromatic.

First condition is necessary for synchronous acceleration[22]. The eighth orbit is longer, than the seventh one by 1.45 of the RF wavelength to obtain deceleration at the next eight passes through the RF structure. The second make the design more compact. The third condition eliminates coupling of horizontal betatron and longitudinal motions and makes focusing more flexible. The splitting magnets are round. The quadrupoles into the 180-degree bends makes each of these bends achromatic. The quadrupoles at the long straight sections are optimized to focus properly both accelerating and decelerating beams.

The length of the straight sections was chosen such, that, when the electron bunches are injected at every eighth period of the RF voltage (e.g. with a frequency of 22.5 MHz), the bunches under acceleration and deceleration are not overlapping each other on the common track, but fill all available equilibrium phases homogeneously. In this case the interaction of the electron bunches, having various energies, decreases dramatically.

Computer simulations of the longitudinal and transverse beam dynamics show that the microtron - recuperator is capable to operate with an average current above 0.1 A. The final bunching occurs on the last track, and that allows to achieve a high peak current (about 100 A) without significant emittance degradation.

3.3 The FEL magnetic system

The scheme of FEL, with the electron outcoupling[27] is shown in Fig. 8. The FEL-oscillator is the optical klystron with undulators 1 and 3, dispersive section 2 and mirrors 6. The microbunched (in the FEL-oscillator and the bend 4) electron beam passes through radiator 5. As the electron beam in the radiator is deflected from the optical cavity axis, the coherent undulator radiation leaves the cavity.

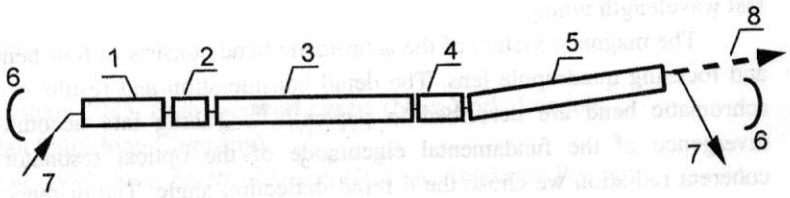

Fig. 8: The scheme of the FEL. 1 – first undulator; 2 – dispersive section; 3 – second undulator; 4 – achromatic bend; 5 – undulator-radiator; 6 – mirror;7 – electron beam; 8 – coherent undulator radiation.

As the FEL is used here only to bunch the electron beam, it has to be optimized for minimal intensity of light on the mirror surfaces. To limit the intracavity power it is convenient to choose a high value of longitudinal dispersion of the dispersive section. In addition, it is preferable to have the second undulator sufficiently longer than the first one. Then «useful» energy modulation in the second undulator, which causes the density modulation in the radiator, is significantly more than «harmful» modulation in the first undulator, which increases the effective energy spread in the radiator. To minimize this increase of the effective energy spread, the intracavity power loss must be minimized (so, mirror reflectivity has to be good).

The actual magnetic system of the FEL consists of four undulators, two bunchers (dispersive sections), and one achromatic bend. The first three undulators and two dispersive sections compose the optical klystron using as a master oscillator. The optical resonator of about 79 m length consists of two mirrors. The number of periods in each undulators is 36, length of the period is 9 cm. To simplify the wavelength tuning we use electromagnetic undulators with the maximum of deflection parameter K about 2. The reason for using of two dispersive sections is to improve the frequency selectivity. To make it clear, consider the two-undulator optical klystron. Let s is the delay of an electron, passing from the middle of the first undulator to the middle of the second one, with respect to the wavefront of light, propagating between these two points (s is also the delay between the wavetrains, emitted by an electron in undulators). The maximum amplification takes place at the

wavelengths λ, which satisfy the condition $s=(n-1/4)\lambda$, where n is the integer. If there are two bunchers and three undulators, we must satisfy two similar conditions simultaneously (for two different s_1 and s_2) to obtain the maximum. Therefore, the maxima will occur more rarely. Such a configuration offers fine and fast wavelength tuning.

The magnetic system of the achromatic bend consists of four bending magnets and focusing quadrupole lens. The detail consideration and results of tests of such achromatic bend are described in papers[27, 28]. Taking into account the angular divergence of the fundamental eigenmode of the optical resonator and of the coherent radiation we chose the 4 mrad deflection angle. The distance between the center of the mirror and coherent radiation axis is 14 cm. The fourth undulator (radiator) is the same, as the previous three, but with slightly lower field amplitude (it is easy, as the undulators are electromagnetic) to maximize the output power[29].

For the initial operation we have chosen the simplest two-mirror optical resonator. Its large length decrease the light intensity on the mirror surfaces and makes possible to obtain oscillation with a low (2 MHz) repetition frequency of the electron bunches. Therefore, we will have a low average power (and therefore, negligible heating of the mirrors), while the peak power will be high. After that we will be able to increase the average power, increasing the repetition rate of the injector pulses.

The FEL radiation will consist of pulses with 10-30 ps duration, 2-22.5 MHz repetition rate, and 2-10 micron wavelength.

3.4 The current status

The building update is finished now. The 2-MeV electron injector was installed and commissioned recently. The assembly of the RF generators and manufacturing of the RF cavities for the main accelerating structure are in progress.

4 Other FEL-related activity

Our last optical klystron OK-4 was transferred from VEPP-3 to the storage ring of Duke university (USA) in 1995. Now this FEL is in operation[30], obtaining the shortest wavelength 0.22 micron.

The 8-MeV microtron and the undulator for the compact far infrared FEL where build for the Korea Atomic Energy Research Institute[31]. They where commissioned successfully and the spontaneous undulator radiation was detected this spring.

The use of the recirculating accelerator-recuperator with long undulator at the last orbit as the high brightness X-ray source was proposed by G. N. Kulipanov recently[32]. The feasibility study is under way now.

We also participate in the SASE ultraviolet range FEL[a] project[33] in the Argonne National Laboratory (USA).

5 References

1. T. C. Marshall, 1985, *Free-Electron Lasers* (New-York, London: Macmillan Publishing Company).
2. C. A. Brau, 1989, *Free-Electron Lasers* (Boston: Academic Press).
3. L. R. Elias et al., 1976, *Phys. Rev. Lett.* **36**, 710.
4. V. N. Baier and A. I. Milstein, 1978, *Phys. Lett.* **65A**, #4, 319.
5. A. N. Skrinsky and N. A. Vinokurov, 1977, *Preprint INP 77-59* (Novosibirsk: INP).
6. V. L. Ginzburg, 1947, *Izv. AN SSSR (Phys.)* **11**, 165; *DAN SSSR* **56**, 145.
7. A. N. Skrinsky and N. A. Vinokurov, 1977, *Preprint INP 77-67* (Novosibirsk: INP).
8. A. N. Skrinsky and N. A. Vinokurov, 1979, in *Proc. 6th Nat. Conf. on Charge Particle Accelerators*, **2** 233 (JINR, Dubna).
9. A. S. Artamonov et al., 1980, *Nucl. Instr. and Meth.* **177**, 247.
10. G. A. Kornyukhin et al., 1983, *Nucl. Instr. and Meth.* **208**, 281.
11. G. A. Kornyukhin et al., 1985, *Nucl. Instr. and Meth.* **237**, 189.
12. N. G. Gavrilov et al., 1989, *Nucl. Instr. and Meth.* **A 282**, 422.
13. I. B. Drobyazko et al., 1989, *Nucl. Instr. and Meth.* **A 282**, 424.
14. M.-E. Couprie et al., 1991, *Nucl. Instr. and Meth.* **A 308**, 39.
15 G. N. Kulipanov et al., 1993, *Nucl. Instr. and Meth.* **A 331**, 98.
16. V. M. Popik and N. A. Vinokurov, 1993, *Nucl. Instr. and Meth.* **A 331**, 768.
17. A. Renieri, 1979, *Nuovo Cimento* **B53**, 160.
18. G. Dattoli and A. Renieri, 1980, *Nuovo Cimento* **B59**, 1.
19. N. A. Vinokurov, Nucl. Instr. and Meth. A 308 (1991) 24.
20. A. N. Skrinsky and N. A. Vinokurov, 1978, *Preprint INP 78-88* (Novosibirsk: INP).
21. T. I. Smith et al., 1987, *Nucl. Instr. and Meth.* **A 259**, 1.

---

[a] The SASE FEL was theoretically described by A. M. Kondratenko and E. L. Saldin[34].

22. R. E. Rand, 1984, *Rerciculating Electron Accelerators* (Harwood Academic Publishers).
23. N. G. Gavrilov et al., 1991, *IEEE J. Quantum Electron.*, **QE-27**, 2626.
24. N. A. Vinokurov et al., 1997, *Proc. of SPIE*, **2988**, 221.
25. N. G. Gavrilov et al., 1993, *Nucl. Instr. And Meth.* **A 331**, ABS17.
26. V.S. Arbuzov et al., 1993, *Proc. 1993 Particle Accelerator Conf. PAC 93, v.***2**, 1226.
27. G.N. Kulipanov et al., IEEE J. Quantum Electron., QE-27, pp. 2566-2568, 1991.
28. N.G. Gavrilov et al., IEEE J. Quantum Electron., QE-27, pp. 2569-2571, 1991.
29. G.N. Kulipanov et al., Nucl. Instr. And Meth. A 375 (1996) 576.
30. V.N. Litvinenko et al., Phys. Rev. Lett. Vol. 78, No. 24, p. 4569 (1997).
31. S.V. Miginsky et al., 1997, *Free electron laser and its application in Asia*, 173.
32. G.N. Kulipanov et al., to be published in J. Synchrotron Rad. 5 (1998).
33. N.A. Vinokurov et al., Proc. of SPIE Vol. 2988, p. 64 (1997).
34. A. M. Kondratenko and E. L. Saldin, 1980, *Part. Acc.* **10**, 207.